



**HAL**  
open science

## Experimental identification of Cohesive Zone Models from thermo-mechanical imaging techniques

Shuang Wen, Yann Monerie, Bertrand Wattrisse, Laurent Sabatier

► **To cite this version:**

Shuang Wen, Yann Monerie, Bertrand Wattrisse, Laurent Sabatier. Experimental identification of Cohesive Zone Models from thermo-mechanical imaging techniques. PhotoMechanics 2013, May 2013, Montpellier, France. pp.Clé USB. hal-00836335

**HAL Id: hal-00836335**

**<https://hal.science/hal-00836335>**

Submitted on 20 Jun 2013

**HAL** is a multi-disciplinary open access archive for the deposit and dissemination of scientific research documents, whether they are published or not. The documents may come from teaching and research institutions in France or abroad, or from public or private research centers.

L'archive ouverte pluridisciplinaire **HAL**, est destinée au dépôt et à la diffusion de documents scientifiques de niveau recherche, publiés ou non, émanant des établissements d'enseignement et de recherche français ou étrangers, des laboratoires publics ou privés.

# EXPERIMENTAL IDENTIFICATION OF COHESIVE ZONE MODELS FROM THERMOMECHANICAL IMAGING TECHNIQUES

S. Wen<sup>1,2,3</sup>, Y. Monerie<sup>2,3</sup>, B. Wattrisse<sup>1,2</sup> and L. Sabatier<sup>1</sup>

<sup>1</sup> Mechanics and Civil Engineering Laboratory, University of Montpellier 2, Pl. E. Bataillon, Montpellier, France

<sup>2</sup> Micromechanics and Structural Integrity Laboratory, IRSN–CNRS–UM2, France

<sup>3</sup> Institute for Radiological Protection and Nuclear Safety, CE Cadarache, bat. 702, BP3-13115 Saint-Paul-lez-Durance Cedex, France

shuang.wen@univ-montp2.fr, yann.monerie@irsn.fr, bertrand.wattrisse@univ-montp2.fr, laurent.sabatier@univ-montp2.fr

**ABSTRACT:** In recent years, cohesive zone models (CZMs) have been developed and widely used in numerical simulations to account for crack initiation and propagation in different materials and structures. This study is focused on the modeling of the elastoplastic damageable behaviour of ductile materials. The damage is associated with a cohesive behaviour of the interface between the purely elastoplastic solid elements. The recent developments in imaging techniques allow reaching local measurement fields (e.g. displacement, strain, strain rate, temperature,...). Under certain assumptions, these measurements allow us to get the distributions of local thermomechanical fields. These distributions can be used to identify the shape and the parameters of the CZM, and then ensure the thermomechanical consistency of this identified model.

## 1. INTRODUCTION

CZMs, which were first introduced in the 1960s through the work of Dugdale [1] and Barenblatt [2], are often written in a mechanical framework introducing a displacement “jump” related to the virtual opening of the crack. In the finite element framework, CZMs are introduced at interfaces between adjacent elements of a finite element discretization. They have been successfully used to simulate fracture in a wide range of materials and to account for heterogeneities at various scales from the grain up to the structure [3].

Although CZMs are becoming increasingly powerful, the identification of these models still remains a delicate issue. In this work, we propose to split the overall elastoplastic damageable behaviour of the ductile material into a purely elastoplastic behaviour related to the bulk response (hardening) and a purely damageable behaviour associated with the cohesive zone (softening). This paper aims to propose an experimental methodology to enhance the choice of CZM constitutive equations and improve their identification. This methodology assumes neither the shape of CZM nor the predefined crack path, but focuses on the experimental validity of the projection of volumic (micro) damage onto a simple surface damage.

The identification procedure involves two steps. The first one consists in characterizing the shape and the parameters of the cohesive zone on tensile test by analysing the kinematic fields locally developed. The measurement of these kinematic fields can be obtained by Digital Image Correlation (DIC). The second one consists in checking the thermo-mechanical consistency of the identified model by confronting the calorimetric measurements deduced from temperature fields with the previsions of the identified model. Temperature fields can be given by Infrared Thermography (IRT),

In the follows, the experimental setup is described firstly, and then some recent results illustrate the potentiality of the experimental approach.

## 2. EXPERIMENTAL SETUP

The experimental setup includes a mechanical test machine, infrared camera and four stereo cameras (Figure 1). The infrared camera is set perpendicularly to the flat specimen surface.



Figure 1- Experimental setup

Each acquisition system is controlled by a separate computer. A specific electronic device was designed to synchronize the frame grabbing of the different systems. The analogical signals provided by the machine sensors (force, displacement) are digitized, and the time is given, on each acquisition computer, by a common clock.

Before starting the tests, the specimen surfaces are speckled with black and white paints in order to obtain the local optical signature, which is necessary to perform DIC.

The two stereoscopic systems allow us to obtain the three components of the displacement field on each side of the sample. The 3D displacement measurement procedure involves three steps [4]. The first step is calibration: determining the intrinsic parameters (lens center, focal length, distortion...) of each camera and the extrinsic parameters (relative position and orientation of the camera) related to the different cameras. The second step is stereo-matching: characterizing the spatial correspondences between pairs of images. The last step is triangulation: determining the 3D coordinates of the physical points from their image coordinates. In our case, the 3D displacement field is directly provided by the "Vic3D" software. Each stereoscopic device allows us to obtain the 3D displacement field in its own coordinate system on one each side of the sample.

A specific procedure has been developed to determine each component of the depth-averaged strain field. In our case, the strain components were derived from the displacement data by a numerical differentiation method based on a local polynomial approximation of the displacement field. The principle to get the 3D strain field is as follows. First, the displacement field provided by each stereoscopic device is expressed in the same coordinate frame. Then, a set of neighbouring points is selected on both specimen surfaces for each measurement point. Finally, by assuming a linear displacement variation through the thickness, an approximation function is determined with the 3D displacement measurements of these neighbouring points, and the depth-averaged 3D strain measurements can be derived from this approximation function.

The infrared camera detects the thermal radiations and then records them as the digital level. With the image provided by the IR camera, the temperature variations of the specimen surface were determined using a pixel calibration protocol [5]. Then the heat sources involved in the material transformation can be estimated using a polynomial approximation of the temperature field, *via* the local heat equation.

In order to compare the kinematic fields with the calorimetric fields, it is necessary to determine the spatial correspondences of the different systems by using a calibration target. Here, we compare the stereo and infrared images of the target (Figure 2). The rigid body movements and the scale factor ratios between the two cameras are taken into account. Eight coordinates (four points) are needed to determine the spatial correspondences with our model.

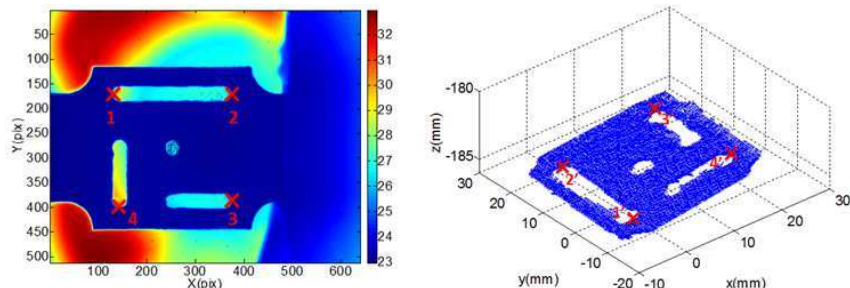


Figure 2- Calibration target: IR image (left); stereo image (right).

### 3. IDENTIFICATION OF COHESIVE ZONE MODELS

The damageable elastoplasticity material behaviour is studied in this work. This material behaviour is described with the superposition of an isochoric elastic-plastic behaviour (bulk part) and a softening surface behaviour (cohesive zone), representing the damage effect of the material. As soon as strain and damage localize, the sample response must be considered as a combination of structural and material effects. A protocol was proposed to derive the uniaxial cohesive zone response associated with the loading direction during a tensile test.

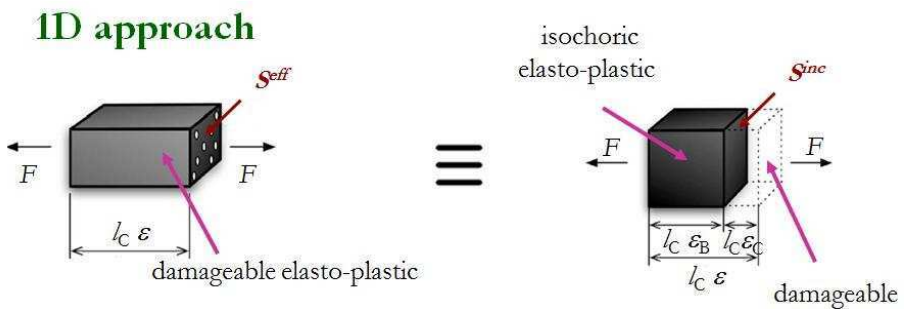


Figure 3- Basic sketch of the strain partition

The Figure 3 represents the basic stretch of the strain partition used to deduce the bulk and the cohesive zone responses from the material response obtained experimentally:

$$\epsilon = \epsilon_B + \epsilon_C \tag{1}$$

Where  $\mathcal{E}$ ,  $\mathcal{E}_B$  and  $\mathcal{E}_C$  are overall tensile axial, bulk and cohesive strain respectively.

In order to describe the mechanical behaviour (material, bulk and cohesive zone), the stress was calculated. The local axial Cauchy stress  $\sigma$  was obtained from the transverse strains ( $\mathcal{E}_2, \mathcal{E}_3$ ), the initial section ( $S_0$ ) and force ( $F$ ):

$$\sigma = F / S_0 e^{(\mathcal{E}_2 + \mathcal{E}_3)} \quad (2)$$

The uniaxial effective stress  $\sigma_{eff}$  was computed by introducing a damage variable ( $D$ ). Here, the damage parameter was associated with volume variations ( $dv_v / dV$ ) measured by DIC and an isotropic damage model:

$$\sigma_{eff} = \sigma / (1 - D) \text{ with } D = (4/3)^{2/3} \pi^{1/3} (dv_v / dV)^{2/3} \quad (3)$$

The bulk response was associated with the incompressible stress  $\sigma_{inc}$ , which can be determined from the tensile strain.

$$\sigma_{inc} = F / S_0 e^{-\mathcal{E}} \quad (4)$$

This method has been applied on different ductile materials (Dual Phase steel and copper). Figure 4 shows the mechanical responses in the localization zone for a tensile test of steel: the overall material response  $\sigma - \mathcal{E}$ , the virtual isochoric response  $\sigma_{inc} - \mathcal{E}_B$  and the surface response  $\sigma - \mathcal{E}_C$ .

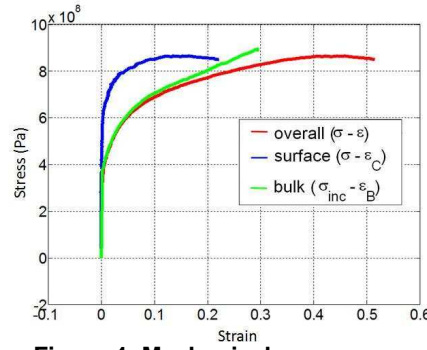


**Figure 4- Mechanical responses**

The bulk behaviour ( $\sigma_{inc} - \mathcal{E}_B$ ) should be resolved at the Gauss points in a Finite Element Method (FEM) and therefore it should be used for determining the bulk parameters of constitutive equations. The identified surface behaviour ( $\sigma - \mathcal{E}_C$ ) can't be directly used in CZM-based simulations. A characteristic length is necessary to transform this softening surface behaviour into a stress-displacement jump cohesive law. The characteristic length can be identified by the following steps: first, a numerical simulation was accomplished with a given cohesive law; then a surface behaviour was obtained from the results of this simulation (the force and the displacement field); finally, the characteristic length can be calculated by matching the given cohesive law and the identified surface behaviour.

#### 4. THERMOMECHANICAL ANALYSIS

The thermodynamic consistency of the model can be validated by using energy balances. The intrinsic dissipation  $w_d$  was computed as the difference between the overall heat source  $w_{ch}$  and the heat source related to the thermoelastic coupling source  $w_{the}$ :

$$w_d = w_{ch} - w_{the} \quad (5)$$

The dissipation associated with damage  $w_d^{coh}$  was estimated from the cohesive law by assuming that the cohesive energy is dissipated completely. The dissipation associated with plasticity  $w_d^{vol}$  can be measured as the difference between the total dissipation and the damage dissipation:

$$w_d^{vol} = w_d - w_d^{coh} \quad (6)$$

In the other hand, this plastic dissipation  $w_d^{vol}$  can be also estimated from the bulk response if the thermo-mechanical behaviour of material is known. The thermo-mechanical consistency of the identified model can be then checked by comparing the plastic dissipation obtained from the measurements and the bulk responses respectively.

In this first approach, the thermo-mechanical behaviour was described using simple rheological model (Figure 5). Here, the elasticity ( $E$  : young's modulus), the plasticity ( $K_i$  : hardening modulus;  $\sigma_i$  : yield strength) and the damage ( $ZC$ ) are taken into account.

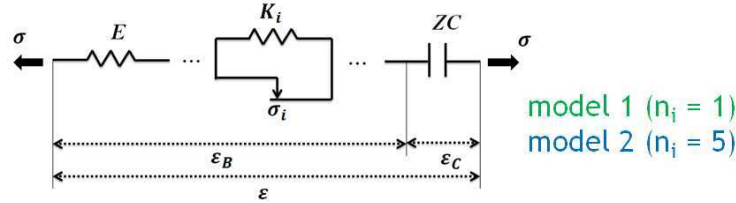


Figure 5- Mechanical responses

Matching the kinematic and calorimetric responses enables us to validate the thermomechanical consistency of the proposed approach. Figure 6 (left) shows the material behaviour obtained by experimentation and two different models ( $n_i=1$  and  $n_i=5$ ). Both models provide the same mechanical behavior, which is consistent with the experimental measurement. But their thermo-mechanical behaviour is different (Figure 6: center, right):

$$d_1^{\text{mod}1} = \sigma_1 \dot{\epsilon}_p \text{ and } d_1^{\text{mod}2} \approx \sigma \dot{\epsilon}_p \quad (6)$$

That means the thermo-mechanical response of the bulk part can be modified without changing its mechanical response. So by modifying the thermo-mechanical model and its parameters, it is possible to obtain a material model, whose thermomechanical response can be consistent with the measurements.

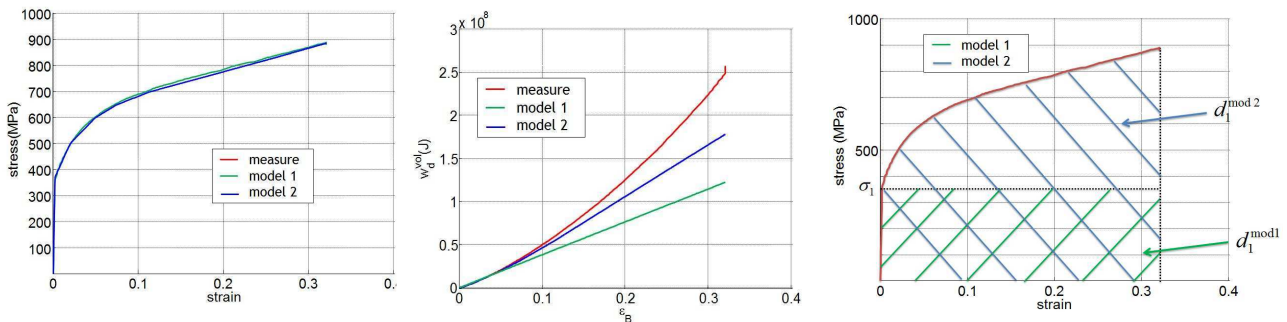


Figure 6- Model comparison: mechanical behaviour (left); thermo-mechanical behaviour (centre); intrinsic dissipation (right)

## 5. CONCLUSION

In order to describe the damaging behaviour of ductile materials, an experimental protocol was developed for the identification of cohesive models. The experiment setup of the identification procedure equipped with several cameras allows us to acquire visible and infrared images. The displacement, strain and temperature fields can be computed from these images by using Digital Image Correlation and Infrared Thermography. Based on the experimental measurements, the identification of cohesive zone models as well as the thermomechanical consistency of the identified model has been discussed. The potentiality of this experimental protocol has been confirmed by several results.

## 6. REFERENCES

1. Dugdale, D.S. (1960) Yielding of steel sheets containing slits. *J. of the Mech. and Ph. of Sol.*, 8, 100-104.
2. Barenblatt, G.I. (1962) The mathematical theory of equilibrium of cracks in brittle fracture. *Adv. Appl. Mech.*, 7, 55-129.
3. Perales, F., Monerie, Y., Dubois, F. and Stainier, L. (2005). Computational non-smooth fracture dynamics in nonlinear and heterogeneous materials. Application to fracture of hydrided Zircaloy. In: Zhou, Yu and Xu (eds.), *Structural mechanics in reactor technology*, 18, Atomic Energy Press, Beijing, China.
4. Sutton, M.A., Orteu, J.J. and Schreier, H.W. (2009). Image Correlation for Shape, Motion and Deformation Measurements. *Hardcover*.
5. Honorat, V., Moreau, S., Muracciole, J.M., Wattrisse B. and Chrysochoos, A. (2005). Calorimetric analysis of polymer behaviour using a pixel calibration of an IRFPA camera. *Int. J. Quantitative Infrared Thermogr.* 2, 153-172.